

# Data Fusion for Displacement Estimation and Tracking of UAV Quadrotor in Dynamic Motion

Lasmadi<sup>1\*</sup>, Denny Dermawan<sup>1</sup>, Muhamad Jalu Purnomo<sup>2,3</sup>

<sup>1</sup>Department of Electrical Engineering, Institut Teknologi Dirgantara Adisutjipto, Indonesia

<sup>2</sup>Department of Material Science and Engineering, National Dong Hwa University, Hualien, Taiwan

<sup>3</sup>Department of Aeronautics, Institut Teknologi Dirgantara Adisutjipto, Indonesia

---

## Article Info

### Article history:

Submitted July 31, 2023

Accepted August 22, 2023

Published August 24, 2023

---

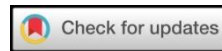
### Keywords:

Data fusion,  
Quadrotor,  
Navigation

---

## ABSTRACT

*The fusion of MIMU and GPS data is generally used to estimate the displacement and tracking of quadrotor UAVs. Meanwhile, displacement estimation inaccuracies during dynamic motion often occur. This error is caused by noise and limited sensor sampling rate especially occurs when the quadrotor changes its attitude rapidly to generate an instantaneous horizontal force. This paper proposes data fusion based on Kalman filter to estimate orientation and displacement. Experiments were also carried out to verify displacement accuracy, i.e. in single-axis and multi-axis sensor motions. The algorithm combines data from MIMU and GPS sensors so that acceleration data is filled in points where GPS data is not available. With this method, the predicted displacement from the MIMU sensor can be corrected every second with data from the GPS and produce accurate displacement and trajectory estimates.*



---

## Corresponding Author:

Lasmadi,

Department of Electrical Engineering, Adisutjipto Institute of Aerospace Technology,

Jl. Majapahit (Janti) Blok R, Lanud Adisutjipto, Yogyakarta, Indonesia.

Email: \*lasmadi@itda.ac.id

---

## 1. INTRODUCTION

Over the last decade, significant progress has been made in aerial robotic vehicles and related technologies, leading to a wide range of potential applications such as emergency response, traffic monitoring, power cable inspection, package delivery, etc. [1]. Quadrotor design and technology have been able to achieve high dynamic maneuverability due to its compact size, simple mechanical system, vertical takeoff/landing capability [2][3], and autonomous landing [1]. Currently, almost all UAVs are equipped with global positioning system (GPS) receivers in order to accurately provide their absolute location. Several factors contribute to the UAV's positioning performance, in terms of its displacement, for example, satellite clock/orbit bias, thermal noise at the receiver, and atmospheric delay. In addition, GPS signals are sensitive to interference and fraud and may be unreliable in congested environments [4].

A navigation system is needed in a UAV to estimate orientation and track its position. Navigation systems generally exploit data from a magneto inertial measurement unit (MIMU) formed by a three-axis gyroscope, three-axis magnetometer, and three-axis accelerometer. On the other hand, for low-cost systems, inertial sensors based on micro-electro-mechanical (MEMS) systems have been widely used. However, low-cost systems with MEMS sensors have the potential to have greater errors in reporting the orientation of the UAV due to increased noise and sensor drift [5][6].

Single sensor-based navigation systems find it difficult to provide robust, accurate, and seamless solutions, due to their limitations. For example, the Inertial Navigation System (INS) is a relative positioning technology and only provides an accurate solution for a limited time, because inertial sensor error and integration error will cause the solution to deviate. Therefore, other sources of absolute positioning data are needed, such as Global Navigation Satellite System (GNSS); however, although accurate in open sky environments, they suffer from signal blockage and multipath in urban areas and other challenging environments [7].

Data fusion via Kalman filters has become a classic approach to dealing with noisy and perturbed measurements. This filtering method primarily combines measurements of different sensors with a dynamic model of the state to be estimated to achieve greater accuracy than would be obtained using standalone sensors. In this case, the Kalman filter integrates data from the gyroscope and accelerometer with the balance between the two sensors used. The Kalman filter algorithm runs in two steps: the first step is the prediction of the state

vector associated with the propagation through the system dynamics model. Then, the second step is the measurement of the data obtained by the sensor to improve predictions to achieve optimal estimation values. Corrections are made by weighting the predicted values according to the measured values and associated uncertainties [8] by setting the measurement noise covariance (R) to imply the weight between the measurement update and the system prediction.

Previous studies reported that orientation can be obtained precisely from accelerometer and magnetometer data when both sensors are static. However, in dynamic conditions, orientation predictions can be made more precisely by using gyroscope sensor data [9][10][11]. To create a robust navigation system, data fusion based on Kalman filters is performed to estimate the orientation of the accelerometer, magnetometer and gyroscope sensors. The filter will improve orientation by giving higher weight to the data from the accelerometer and magnetometer sensors when the quadrotor is in static conditions to improve accuracy [10][12].

Acceleration data from GPS sensors can be combined to estimate quadrotor position by integrating data from INS (inertial navigation system) and GPS through Kalman filters. INS data is used for prediction purposes, while GPS data is for measurement. In previous studies, by setting the measured noise covariance, the Kalman filter combines data from the accelerometer and GPS sensors where available, otherwise using data only from the accelerometer sensor.

This paper provides accurate tracking of the quadrotor's trajectory during maneuvers. This research focuses on the cross-configuration quadrotor, where this configuration can provide higher torque to increase maneuverability. This research develops a quadrotor orientation determination and translation method. Two processes based on the Kalman filter are carried out on the system, first determining the orientation using the Kalman filter and then secondly determining the translation using another Kalman filter [10]. This research combines the two processes to increase robustness and accuracy.

## 2. RESEARCH METHOD

This paper proposes data fusion based on Kalman filter to estimate the orientation and displacement of the quadrotor. This method is accomplished by integrating the accelerometer, gyroscope, magnetometer, and GPS sensor without rebuilding the entire filter structure. The basic formulation is described as follows:

The state vector is predicted from the state dynamic equation can be written as a linear equation as formula (1).

$$\hat{x}_k = Ax_{k-1} + Bv_k \quad (1)$$

where  $x$  is the state vector consisting of the quadrotor's orientation  $\omega$  and three-dimensions displacement  $r$  as

$$x = [\omega \ r]^T \quad (2)$$

The subscript  $k$  denotes the  $k$ -th epoch, the subscript  $-$  denotes the state vector estimate after the state propagation. The symbol  $\omega$  depicts the orientation that contains roll ( $\phi$ ), pitch ( $\theta$ ), and yaw ( $\psi$ ) angles and their angular rates as follow.

$$\omega = [\phi \ \dot{\phi} \ \theta \ \dot{\theta} \ \psi \ \dot{\psi}] \quad (3)$$

Meanwhile  $r$  shows the three-dimensional displacement in  $x$ -axis ( $x$ ),  $y$ -axis ( $y$ ), and  $z$ -axis ( $z$ ) and followed by their velocity and acceleration,

$$r = [x \ y \ z \ \dot{x} \ \dot{y} \ \dot{z} \ \ddot{x} \ \ddot{y} \ \ddot{z}] \quad (4)$$

The  $A$  is the system propagation model and  $B$  is the matrix contains coefficients of the input terms. They are respectively a combined model of  $A_{ori}$  and  $A_{trans}$ ,  $B_{ori}$  and  $B_{trans}$  from Ref [1] as follows,

$$A = \begin{bmatrix} A_{ori} & 0_{6 \times 9} \\ 0_{9 \times 6} & A_{trans} \end{bmatrix} \quad (5)$$

$$B = \begin{bmatrix} B_{ori} & 0_{6 \times 3} \\ 0_{9 \times 3} & B_{trans} \end{bmatrix} \quad (6)$$

where  $0_{i \times j}$  is the  $i$ -row and  $j$ -column zero matrix.

Then,  $v$  is the system input provided by the INS. This contains angular rates taken from gyroscope and the acceleration obtained from accelerometer,

$$v = [\dot{\phi} \ \dot{\theta} \ \dot{\psi} \ \ddot{x} \ \ddot{y} \ \ddot{z}]^T \quad (7)$$

where  $\dot{\phi}$ ,  $\dot{\theta}$ ,  $\dot{\psi}$  are the angular velocities of roll, pitch, and yaw obtained from the gyroscope sensor respectively. Meanwhile,  $\ddot{x}$ ,  $\ddot{y}$ , and  $\ddot{z}$  are the acceleration on navigation frame. These three values are obtained by using the following equation.

$$\begin{bmatrix} \ddot{x} \\ \ddot{y} \\ \ddot{z} \end{bmatrix} = \mathcal{R}^N_B \begin{bmatrix} \ddot{x} \\ \ddot{y} \\ \ddot{z} \end{bmatrix} - g \quad (8)$$

where  $\ddot{x}$ ,  $\ddot{y}$ , and  $\ddot{z}$  are the acceleration on the body frame for the  $x$ ,  $y$ , and  $z$  axes obtained from the accelerometer, and  $\mathbf{g}$  is the acceleration due to gravity. Then,  ${}^N_B\mathcal{R}$  is a rotation matrix that converts values in sensor frames to navigation frames. This matrix takes the attitude from the previous era and is formulated as follows,

$${}^N_B\mathcal{R} = \begin{bmatrix} c\theta_{k-1}c\psi_{k-1} & s\phi_{k-1}s\theta_{k-1}c\psi_{k-1} - c\phi_{k-1}s\psi_{k-1} & c\phi_{k-1}s\theta_{k-1}c\psi_{k-1} + s\phi_{k-1}s\psi_{k-1} \\ c\theta_{k-1}s\psi_{k-1} & s\phi_{k-1}s\theta_{k-1}s\psi_{k-1} + c\phi_{k-1}c\psi_{k-1} & c\phi_{k-1}s\theta_{k-1}s\psi_{k-1} - s\phi_{k-1}c\psi_{k-1} \\ -s\theta_{k-1} & s\phi_{k-1}c\theta_{k-1} & c\phi_{k-1}c\theta_{k-1} \end{bmatrix} \quad (9)$$

where  $c(ang) = \cos(ang)$  and  $s(ang) = \sin(ang)$ .

The predicted state error covariance matrix can be represented by the matrix in equation (10).

$$P_k = AP_{k-1}A^T + Q \quad (10)$$

where  $Q$  is the process noise covariance constructed by the combination of  $Q_{ori}$  and  $Q_{trans}$  from Ref [1].

$$Q = \begin{bmatrix} Q_{ori} & 0_{6 \times 9} \\ 0_{6 \times 9} & Q_{trans} \end{bmatrix} \quad (11)$$

The Kalman gain can be expressed as equation (12),

$$K_k = P_k H^T (H P_k H^T + R)^{-1} \quad (12)$$

The  $H$  is the observation matrix and the  $R$  is the measurement noise covariance. They respectively combine the models  $H_{ori}$  and  $H_{trans}$ ,  $R_{ori}$  and  $R_{trans}$  in Ref [1] as follows,

$$H = \begin{bmatrix} H_{ori} & 0_{9 \times 3} \\ 0_{6 \times 3} & H_{trans} \end{bmatrix} \quad (13)$$

$$R = \begin{bmatrix} R_{ori} & 0_{3 \times 3} \\ 0_{3 \times 3} & R_{trans} \end{bmatrix} \quad (14)$$

The Kalman gain matrix is used to correct predictions with the appropriate amount, as in equation (15).

$$x_k = x_k^- + K_k (Z_k - Hx_k^-) \quad (15)$$

The  $Z$  is the measurement given by the calculation results of current orientation  $Z_\omega$  and displacement  $Z_r$  as follows.

$$Z = [Z_\omega \quad Z_r]^T \quad (16)$$

Orientation contains the attitude and angle of the heading. The attitude angle consists of roll ( $\phi$ ) and pitch ( $\theta$ ) angles which are calculated from the acceleration taken from the accelerometer.

$$Z_\omega = [\phi \quad \theta \quad \psi]^T \quad (17)$$

It is known that the roll and pitch angles are calculated by equations (18) and (19) [2].

$$\phi = \tan^{-1} \left( \frac{\ddot{y}}{\sqrt{\ddot{x}^2 + \ddot{z}^2}} \right) \quad (18)$$

$$\theta = \tan^{-1} \left( \frac{\ddot{x}}{\sqrt{\ddot{y}^2 + \ddot{z}^2}} \right) \quad (19)$$

where  $\ddot{x}$ ,  $\ddot{y}$ , and  $\ddot{z}$  are the acceleration in the  $x$ ,  $y$ , and  $z$  axes read by the accelerometer in the sensor frame, respectively. Meanwhile, the heading angle is yaw ( $\psi$ ) which is calculated from the geomagnetic field using equation (20) [1].

$$\psi = \tan^{-1} \left( \frac{{}^{xy}m_y}{{}^{xy}m_x} \right) - \zeta \quad (20)$$

where  $\zeta$  is the magnetic declination and  ${}^{xy}m_i$  is the component of the earth's magnetic field in an  $x$ - $y$  navigation frame. The final value is obtained from the earth's magnetic field which is read by the magnetometer  $m_i$  (in the sensor frame) which has been rotated on the  $x$  and  $y$  axes using the following equation.

$$\begin{aligned} {}^{xy}m_i &= \mathcal{R}_Y(\theta) \cdot \mathcal{R}_X(\phi) \cdot m_i \\ &= \begin{bmatrix} \cos \theta & 0 & \sin \theta \\ 0 & 1 & 0 \\ -\sin \theta & 0 & \cos \theta \end{bmatrix} \begin{bmatrix} 1 & 0 & 0 \\ 0 & \cos \phi & -\sin \phi \\ 0 & \sin \phi & \cos \phi \end{bmatrix} m_i \\ &= \begin{bmatrix} \cos \theta & \sin \phi \sin \theta & \cos \phi \sin \theta \\ 0 & \cos \phi & -\sin \phi \\ -\sin \theta & \sin \phi \cos \theta & \cos \phi \cos \theta \end{bmatrix} m_i \end{aligned} \quad (21)$$

The quadrotor displacement consists of the  $x$ -axis (north-south),  $y$ -axis (east-west), and  $z$ -axis (down-up) in the navigation frame, which can be expressed as,

$$Z_r = [x \quad y \quad z]^T \quad (22)$$

The displacement distance of the quadrotor can be found by calculating the displacement from the origin. This distance can be calculated by determining the difference in degrees of latitude and longitude obtained from the GPS. If the earth is assumed to be spherical, the difference in latitude  $\Delta x$  can be calculated using the following equation.

$$\Delta x = \frac{2\pi r \Delta \alpha}{360} \quad (23)$$

where  $r$  is the radius of the earth = 6,371 kilometer,  $\alpha$  is the degree of latitude, and  $\Delta \alpha$  is different degrees of latitude. Then, the difference in longitude  $\Delta y$  can be expressed using the following equation.

$$\Delta y = \frac{2\pi r \Delta \beta}{360} \cos \alpha \quad (24)$$

where  $\beta$  is the degree of latitude and  $\Delta \beta$  is different degrees of longitude. The current displacement can be calculated as follows,

$$\begin{aligned} x_k &= x_{k+1} + \Delta x \\ y_k &= y_{k+1} + \Delta y \end{aligned} \quad (25)$$

The altitude data from sea level  $Z_k$  is directly obtained from GPS data.

The final step of the Kalman filter algorithm is to update the state error covariance using the following equation (26).

$$P_k = (I - K_k H) P_k^- \quad (26)$$

This algorithm works according to the flowchart shown in Figure 1.

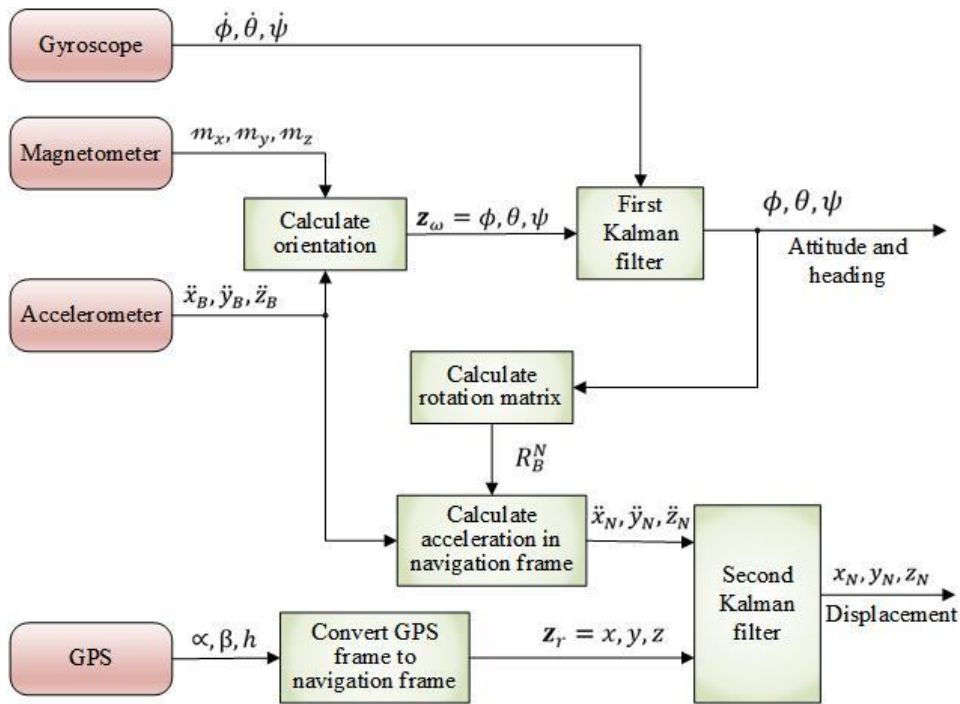


Figure 1. Flowchart diagram of system

As shown in Figure 1, the Kalman filter combines data from the accelerometer, gyroscope, magnetometer, and GPS. Fusing data by Kalman filters is made to estimate the orientation of the accelerometer, gyroscope, and magnetometer sensors. The orientation of the quadrotor is calculated using data from the accelerometer and magnetometer when both sensors are static to obtain accurate data. In dynamic conditions, orientation is predicted more precisely using gyroscope sensor data. Detect static or dynamic conditions using the acceleration-covariance threshold method. Further discussion of this method can be seen in reference [10]. To get higher accuracy, the filter corrects the orientation by giving higher weight to the accelerometer and magnetometer sensor data when the quadrotor is in static condition.

Then the quadrotor displacement is done by combining data of accelerometer and GPS. At this stage, the acceleration that has been converted into a navigation frame is used as prediction data, and the displacement value calculated from the location data obtained from the GPS sensor is used as correction data. Since data from GPS is available only once per second, data fusion gives heavy weight to GPS data when there is new data from

the GPS sensor, whereas the prediction state from acceleration data fills quadrotor displacement when GPS data is not available.

### 3. RESULT AND DISCUSSION

Each sensor has a maximum sampling frequency as shown in Table 1. The acceleration sensor uses a sampling frequency of 202.1 Hz, while the GPS uses a sampling frequency of 1 Hz. With this significant difference, there will be several conditions where the data from the GPS sensor cannot be used correctly to determine the UAV's movement.

Table 1. Sampling-frequency for each sensor

Sensor	Sampling-frequency
Accelerometer	202,1 Hz
Gyroscope	50,8 Hz
Magnetometer	50,8 Hz
GPS	1 Hz

When the UAV maneuvers quickly and causes large changes in acceleration, the displacement data can no longer be correctly corrected by the location data from the GPS. Fault detection of GPS signals has also been investigated in [10]. To illustrate the performance of the proposed algorithm, the quadrotor is programmed to fly from  $t = 1.1$  seconds with a speed of 6 km/hour. The results of this test can be seen in Figure 2.



Figure 2. Sensor data

The quadrotor pitch angle is set to  $-10^\circ$  at  $t = 1.1$  s for 0.1 s to produce forward torque. The change is marked by a change in acceleration and angular velocity as shown in Figure 1. The attitude angle obtained from the Kalman filter output can be seen in Figure 3.

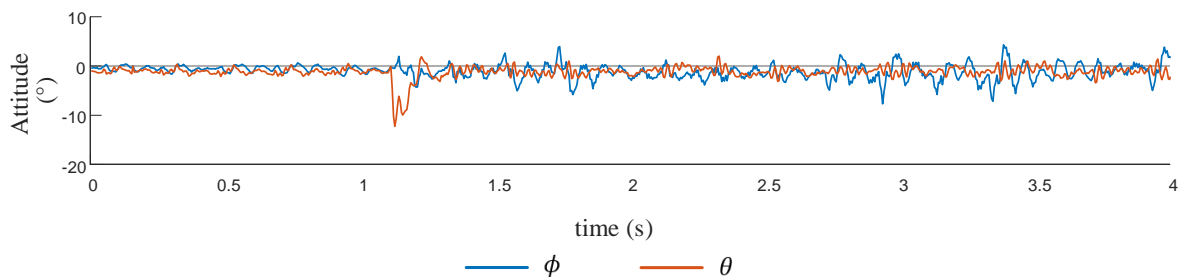


Figure 3. Attitude angle data

The attitude angle is entered into the rotation matrix according to equation (9). Then, by multiplying it with the acceleration data according to equation (8), the resulting acceleration in the navigation frame is obtained.

Thus, a short torque causes a sudden change in acceleration as well as a change in speed and displacement as shown in Figure 4. In this graph, all values are in the navigation frame.

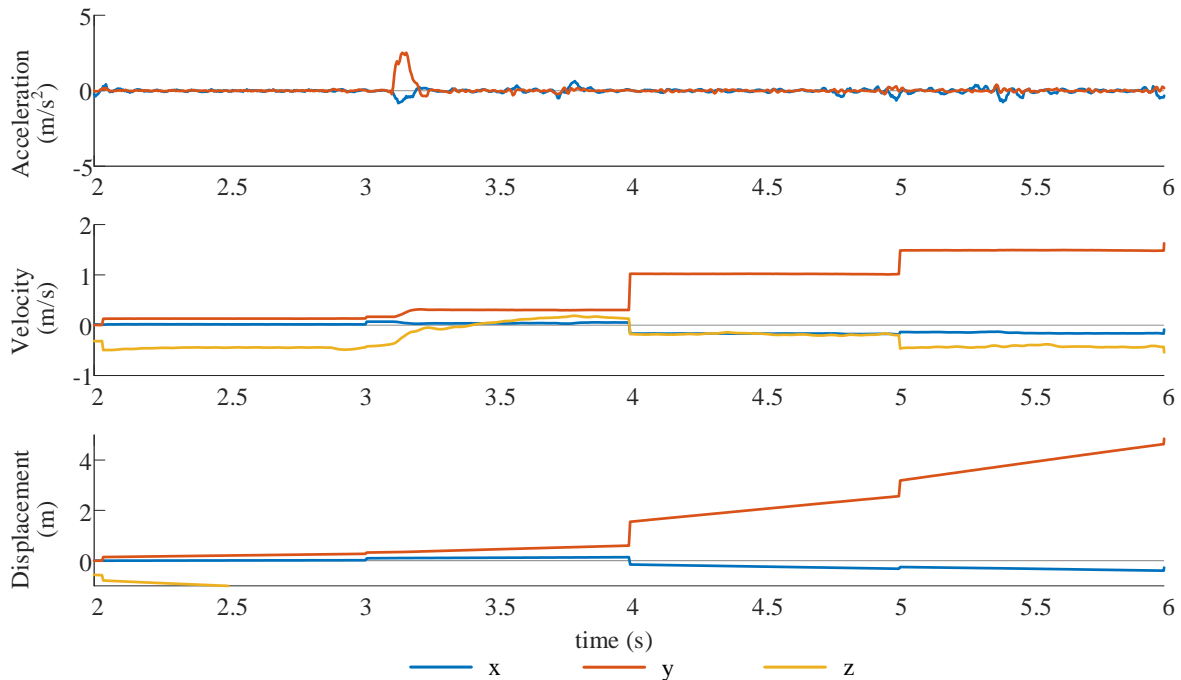


Figure 4. Velocity and displacement data of quadrotor

In Figure 4, it can be seen that the short torque causes an eastward acceleration. Note that in the navigation frame, the  $x$ ,  $y$ , and  $z$  axes indicate north, east, and down (NED) directions, respectively. This acceleration causes a speed of 0.24 m/s so that at  $t = 2$  s, the quadrotor experiences a displacement of 0.2 m to the east. There is GPS data every second. At  $t = 2$  s, the location data from the GPS is used to correct displacement. Based on GPS data, the quadrotor's current displacement is 1 m. This correction has led to an increase in the displacement graph as shown in Figure 4.

Acceleration inaccuracies cause velocity and displacement errors. This can be explained as follows. As mentioned earlier, in dynamic conditions, the Kalman filter uses data from the gyroscope to determine orientation. Because the gyroscope's sample frequency is lower than that of the accelerometer, this orientation angle is subject to error. This causes an error in the estimation of angles by the Kalman filter so that the rotation matrix in equation (9) does not correctly convert each acceleration component on the sensor frame  $(\ddot{x}, \ddot{y}, \ddot{z})$  to a navigation frame  $(\ddot{x}, \ddot{y}, \ddot{z})$ . Therefore, the acceleration on the navigation frame does not reflect the actual conditions. By using data fusion, displacement errors can be corrected every second with GPS data using Kalman filters. The first correction occurs at  $t = 2$  seconds. At  $t = 3$  seconds, displacement is corrected again with data from GPS. At that time the velocity value was also corrected to 1.5 m/s and displacement to 2.8 m.

To illustrate the performance of the proposed algorithm, the quadrotor flies following a rectangular trajectory as shown in Figure 5 with a speed of 6 km/h in 80 seconds. The Quadrotor flies at  $96^\circ$  for 30 meters for  $t = 0 - 18$  seconds. This flight also changed the yaw angle from  $96^\circ$  to  $6^\circ$ . After that, the quadrotor flies in the direction of  $6^\circ$  for 30 meters for  $t = 19 - 37$  seconds while changing the yaw angle from  $6^\circ$  to  $231^\circ$  then flies towards  $231^\circ$  for 30 meters for  $t = 38 - 54$  seconds while changing the yaw angle from  $231^\circ$  to  $186^\circ$ . Furthermore, the last flight to 186 degrees was not followed by a change in yaw angle. Figure 5 shows data from the accelerometer, gyroscope, magnetometer, and GPS. Acceleration, angular velocity, and magnetic field data are in the sensor frame while the displacement data from GPS is in the global frame. Meanwhile, the estimation of acceleration, velocity, and displacement of the quadrotor can be obtained from the output of the Kalman filter as shown in Figure 6.

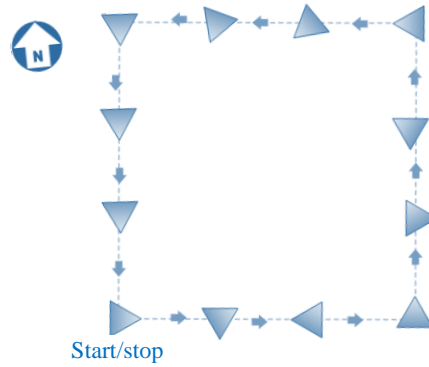


Figure 5. The rectangular trajectory of quadrotor

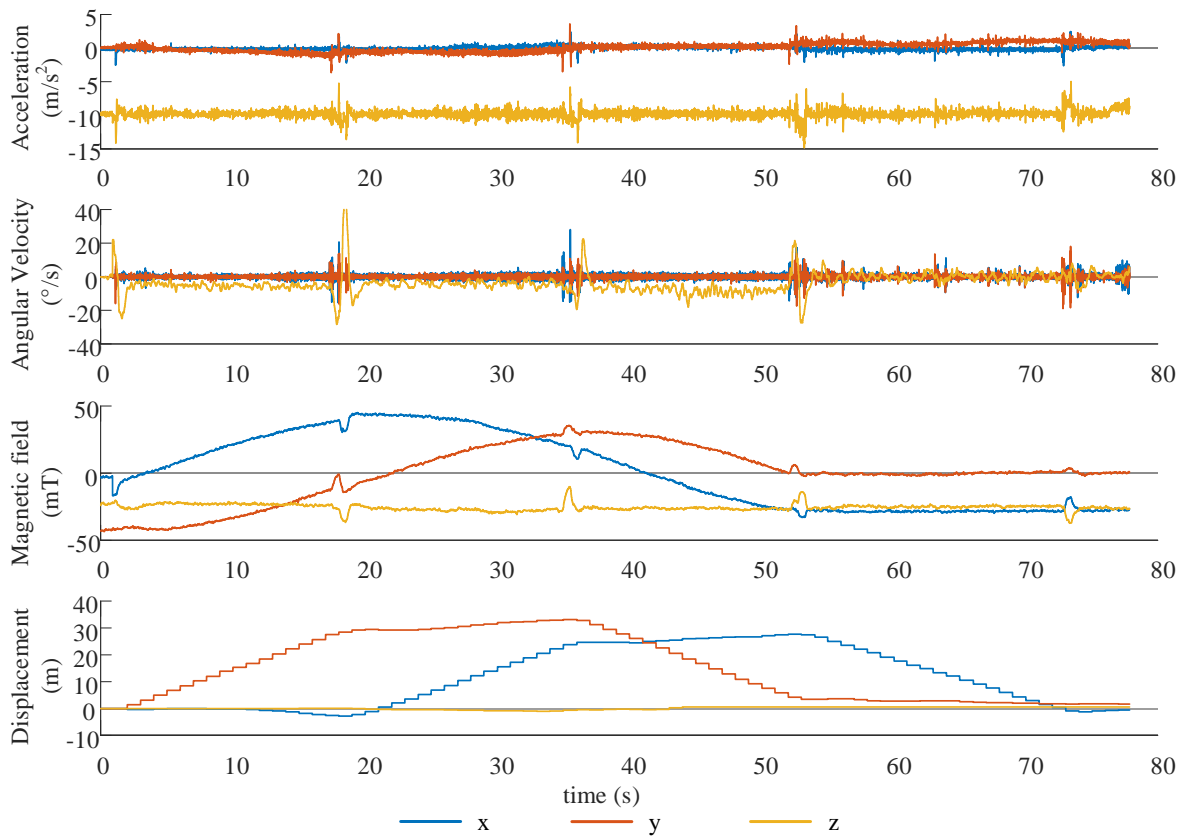


Figure 6. Graph of sensor input data during flight

From comparing the displacement graphs in Figures 6 and 7, it can be shown that by applying data fusion using the Kalman filter, we can obtain a more precise quadrotor displacement. Using only the accelerometer, the displacement of the quadrotor cannot be precise, but the displacement graph has a high resolution because the accelerometer sampling frequency is quite high. While from the GPS data, the quadrotor displacement can be precise, the displacement graph is not high resolution because the sampling frequency is only 1 Hz. By implementing data fusion using a Kalman filter, we can get quite precise displacement data with a high enough resolution. In this case, predictive data from the accelerometer can be entered at points where GPS data is not available.

The results of previous research [10][13], the use of INS and GPS data fusion makes the UAV displacement more precise. However, in this study, by using two Kalman filters to estimate orientation and displacement at the same time, displacement estimation and correction can be performed in one integrated step. The application of Kalman filters also allows further correction algorithms to be made easily [14][15].

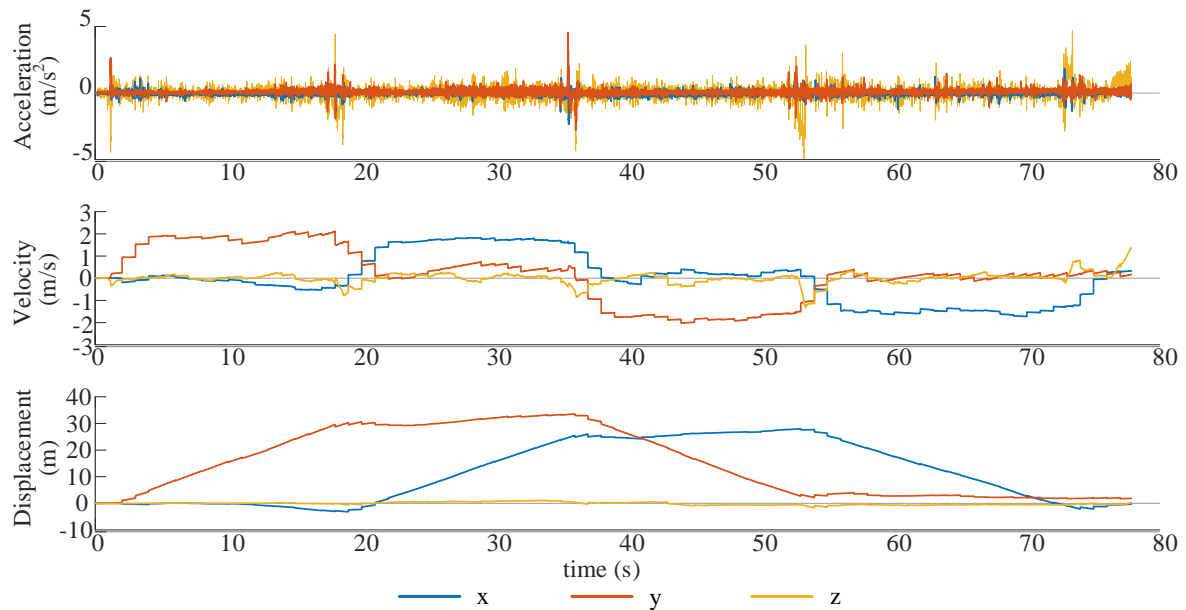


Figure 7. Graphs for quadrotor acceleration, velocity and displacement

#### 4. CONCLUSIONS

In this paper, we propose data fusion to estimate the orientation and displacement of quadrotor UAVs based on Kalman filter. Displacement estimates can be provided by combining data from MIMU and GPS sensors. Accelerometers are capable of providing high-speed data, while GPS sensors can provide high-precision data. Data fusion based on the Kalman filter combines data from both sensors so that acceleration data is filled at points where GPS data is not available. With this method, predictions of speed and displacement from the MIMU sensor can be corrected every second from GPS data to produce accurate estimates of displacement and trajectory.

#### REFERENCES

- [1] X. Liu, S. Zhang, J. Tian, and L. Liu, "An onboard vision-based system for autonomous landing of a low-cost quadrotor on a novel landing pad," *Sensors (Switzerland)*, vol. 19, no. 21, 2019. <https://dx.doi.org/10.3390/s19214703>
- [2] R. Li, Q. Zhu, H. Nemati, X. Yue, and P. Narayan, "Trajectory tracking of a quadrotor using extend state observer based U-model enhanced double sliding mode control," *Journal of the Franklin Institute*, vol. 360, no. 4, pp. 3520–3544, 2023. <https://dx.doi.org/10.1016/j.jfranklin.2022.11.036>
- [3] Y. Wang, X. Lyu, H. Gu, S. Shen, Z. Li, and F. Zhang, "Design, implementation and verification of a quadrotor tail-sitter VTOL UAV," in *2017 International Conference on Unmanned Aircraft Systems (ICUAS)*, 2017, pp. 462–471, 2017. <https://dx.doi.org/10.1109/ICUAS.2017.7991419>
- [4] R. Ghoddousi-Fard and F. Lahaye, "High latitude ionospheric disturbances: Characterization and effects on GNSS precise point positioning," in *2015 International Association of Institutes of Navigation World Congress (IAIN)*, pp. 1–6, 2015. <https://dx.doi.org/10.1109/IAIN.2015.7352231>
- [5] D. A. Grejner-Brzezinska, C. K. Toth, T. Moore, J. F. Raquet, M. M. Miller, and A. Kealy, "Multisensor Navigation Systems: A Remedy for GNSS Vulnerabilities?," *Proceedings of the IEEE*, vol. 104, pp. 1339–1353, 2016.
- [6] A. Nez, L. Fradet, F. Marin, T. Monnet, and P. Lacouture, "Identification of noise covariance matrices to improve orientation estimation by kalman filter," *Sensors (Switzerland)*, vol. 18, no. 10, 2018, <https://dx.doi.org/10.3390/s18103490>
- [7] Y. Zhuang *et al.*, "Multi-sensor integrated navigation/positioning systems using data fusion: From analytics-based to learning-based approaches," *Information Fusion*, vol. 95, pp. 62–90, 2023. <https://dx.doi.org/10.1016/j.inffus.2023.01.025>
- [8] S. Bijjahalli, R. Sabatini, and A. Gardi, "Advances in intelligent and autonomous navigation systems for small UAS," *Progress in Aerospace Sciences*, vol. 115, pp. 100617, 2020. <https://dx.doi.org/10.1016/j.paerosci.2020.100617>



- [9] L. Lasmadi, F. Kurniawan, and M. I. Pamungkas, "Estimasi Sudut Rotasi Benda Kaku Berbasis IMU Menggunakan Kalman Filter," *Aviation Electronics, Information Technology, Telecommunications, Electricals, and Controls (AVITEC)*, vol. 3, no. 1, pp. 57-68, 2021, <https://dx.doi.org/10.28989/avitec.v3i1.909>
- [10] F. Kurniawan, M. R. Erdata Nasution, O. Dinaryanto, and L. Lasmadi, "Penentuan Orientasi dan Translasi Gerakan UAV menggunakan Data Fusion berbasis Kalman Filter," *Aviation Electronics, Information Technology, Telecommunications, Electricals, and Controls (AVITEC)*, vol. 3, no. 2, pp. 99-115, 2021. <https://dx.doi.org/10.28989/avitec.v3i2.890>
- [11] L. Lasmadi, F. Kurniawan, D. Dermawan, and G. N. P. Pratama, "Mobile Robot Localization via Unscented Kalman Filter," in *2019 International Seminar on Research of Information Technology and Intelligent Systems (ISRITI)*, pp. 129–132, 2019. <https://dx.doi.org/10.1109/ISRITI48646.2019.9034570>
- [12] R. B. Widodo and C. Wada, "Attitude Estimation Using Kalman Filtering: External Acceleration Compensation Considerations," *Journal of Sensor*, vol. 2016, 2016. <https://dx.doi.org/10.1155/2016/6943040>
- [13] G. Wang *et al.*, "A GNSS/INS Integrated Navigation Algorithm Based on Kalman Filter," in *IFAC PapersOnLine*, Elsevier B.V., pp. 232–237, 2018. <https://dx.doi.org/10.1016/j.ifacol.2018.08.151>
- [14] G. Zhang and L.-T. Hsu, "Intelligent GNSS/INS integrated navigation system for a commercial UAV flight control system," *Aerospace Science and Technology*, vol. 80, pp. 368–380, 2018. <https://dx.doi.org/10.1016/j.ast.2018.07.026>
- [15] Y. Guo, M. Wu, K. Tang, J. Tie, and X. Li, "Covert Spoofing Algorithm of UAV Based on GPS/INS-Integrated Navigation," *IEEE Transactions on Vehicular Technology*, vol. 68, no. 7, pp. 6557–6564, 2019. <https://dx.doi.org/10.1109/TVT.2019.2914477>